Ductile damage prediction in different cold forming processes

T.-S. CAO [a,b], P.-O.BOUCHARD [b], P. MONTMITONNET [b]

a. ArcelorMittal, Global R&D, Maizières Process, Voie Romaine, BP 30320, F-57283 Maizières-lès-Metz Cedex, France.
b. CEMEF, MINES ParisTech, UMR CNRS 7635, CS 10207, 06904 Sophia-Antipolis Cedex, France.
trongson.cao@arcelormittal.com; pierre-olivier.bouchard@mines-paristech.fr; pierre.montmitonnet@mines-paristech.fr

Abstract

The purpose of the present paper is to show how and to what extent the introduction of refined, shear sensitive models improves on previous ones, based on triaxiality only, for the phenomenological description of ductile damage in bulk cold metal forming processes. Wire-drawing and wire rolling are taken as examples. A set of mechanical tests has been conducted: round bar, notched bar and plane strain tensions as well as torsion for pure shear deformation. Both constitutive and damage models parameters have been carefully identified, with back-computation of the laboratory tests for validation. Application of the models to the cold forming processes, described here, shows the superiority of the shear-enhanced models for locating maximum damage in flat wire rolling, where a significant amount of shear is present ("blacksmith's cross" deformation pattern). On the contrary, it proves unnecessary for low-shear processes such as wire-drawing. The cavity-growth Gurson-Tvergaard-Needleman model, with a modified formulation for nucleation, seems to be the best basis for damage prediction in patented high carbon steel.

Keywords: Ductile damage, metal forming, triaxiality, Lode angle

1 Introduction

In the modern world, products should be produced under low cost and severe environmental constraints, there is thus no longer place for the classical "trial and error" tests. For all industrial cold forming processes, the ability of numerical modeling to predict ductile fracture is crucial. The common issue is to predict ductile damage and fracture in multi-axial and non-proportional loadings involving very large plastic strain, in which the damage may localize away from the maximum critical strain locations. Moreover, the shear effects in several processes are important, damage models thus must be able to capture the associated shear damage mechanism. There is thus real need to develop robust damage models for industrial applications. By robustness, the challenges for a good model are three-fold: (1) physical mechanisms of the onset of damage and fracture must be captured; (2) the models have to be suitable for numerical implementation and must be simple enough for real-scale structure simulations; and (3) models parameters should be convenient for identification for massive applications. The purpose of the present paper is to examine the capacity of different types of models in three approaches of ductile damage (namely, fracture criteria, coupled phenomenological and micro-mechanics based models) to predict damage and fracture in two different processes: wire-drawing and wire rolling.

2 Damage models developments and implementations

Six ductile damage models are compared, which are described in terms of invariants of the stress tensor: the stress triaxiality $\eta = \sigma_m/\overline{\sigma}$; and the Lode parameter $\overline{\theta} = 1 - \frac{6\theta}{\pi} = 1 - \frac{2}{\pi} \arccos\left(\frac{\left(\frac{27}{2}\det(s)\right)}{\overline{\sigma}^3}\right)$ ($\sigma_m, \overline{\sigma}$ are the mean and von Mises equivalent stresses; s is the deviatoric stress tensor). Elasto-plastic hardening law was used combined with J_2 plasticity, except the case of Gurson-like models (section 2.3) where pressure-dependent plasticity model was employed. The hardening law used was a modified form of the Voce law, in which the flow stress is defined as:

$$\sigma_0 = \sigma_{p0} + (\sigma_{ps} - \sigma_{p0} + K_2\overline{\epsilon}_p)(1 - \exp(-n\overline{\epsilon}_p)) \qquad (1)$$

where: σ_0 is the flow stress of material matrix, n and K_2 are material parameters; $\sigma_{p0} = \sigma_0(\bar{\epsilon}_p = 0)$; $\sigma_{ps} = \sigma_0 (\bar{\epsilon}_p \to \infty)$ if $K_2 = 0$. The unit of K_2, σ_{p0} and σ_{ps} is MPa. The identified hardening law was validated for different mechanical tests: compression, torsion and tensile tests ([1, 2]).

2.1 Fracture criterion

The Bai & Wierzbicki fracture criterion was used ([3]), in which the strain to fracture function is defined as:

$$\bar{\epsilon}_f(\eta, \bar{\theta}) = \left[\frac{1}{2} \left(D_1 e^{-D_2 \eta} + D_5 e^{-D_6 \eta} \right) - D_3 e^{-D_4 \eta} \right] \bar{\theta}^2 + \frac{1}{2} \left(D_1 e^{-D_2 \eta} - D_5 e^{-D_6 \eta} \right) \bar{\theta} + D_3 e^{-D_4 \eta} \tag{2}$$

where $D_1, D_2, D_3, D_4, D_5, D_6$ are 6 positive material parameters which need to be identified. A linear incremental relationship is assumed between the damage variable D and the equivalent plastic strain $\bar{\epsilon}_p$:

$$D(\bar{\epsilon}_p) = \int_0^{\bar{\epsilon}_p} \frac{d\bar{\epsilon}_p}{\bar{\epsilon}_f(\eta, \bar{\theta})} \tag{3}$$

2.2 Coupled phenomenological models

Three models were implemented and used: models in Continuum Damage Mechanics (CDM) framework (Lemaitre [4], Lode-dependent Enhanced Lemaitre-LEL [5]) and a fracture strain-based coupled phenomenological model proposed by Xue [6]. The governing equations of the LEL model are summarized as:

$$\dot{D} = \begin{cases} \dot{\bar{\epsilon}}_p \left(\frac{Y}{S} \right)^b \frac{1}{\alpha_1 + \alpha_2 \bar{\theta}^2} & \text{, if } \bar{\epsilon}_p > \epsilon_D = \epsilon_{D0} exp(-A\eta) \quad \text{and} \quad \eta > \eta_{\text{cutoff}} \\ 0 & \text{, otherwise} \end{cases} \tag{4}$$

$$\begin{cases} \bar{\sigma} = w(D)\sigma_M \\ E = w(D)E_M \end{cases} \quad \text{with} \quad w(D) = \begin{cases} 1 - D & \text{, if } \eta \geq \eta_1 \\ 1 - \frac{(1-h)\eta + h\eta_1 - \eta_2}{\eta_1 - \eta_2} D & \text{, if } \eta_1 > \eta \geq \eta_2 \\ 1 - hD & \text{, if } \eta < \eta_2 \end{cases} \tag{5}$$

where $\alpha_1, \alpha_2, \epsilon_{D0}, A, \eta_1, \eta_2$ are additional parameters; η_{cutoff} is the cutoff value of the stress triaxiality to be identified, which could be chosen equal to $-1/3$ from the study of [7] for a first approximation (or taken as a function of the Lode parameter as proposed by [8]). It should be noted that, if $\alpha_2 = 0$, $\alpha_1 = 1$ and $A = 0$, the evolution equation of the original Lemaitre model is retrieved.

Xue ([6]) proposed a phenomenological damage model, which is based on the definition of the equivalent fracture strain ϵ_f as a function of hydrostatic pressure (p) and Lode angle (θ_L):

$$\epsilon_f(p, \theta_L) = \epsilon_{f0} \mu_p(p) \mu_\theta(\theta_L) \quad \text{, with: } \mu_p = 1 - q \ln(1 - \frac{p}{p_L}) \quad \text{and} \quad \mu_\theta = \gamma + (1 - \gamma) \left[\frac{6 |\theta_L|}{\pi} \right]^k \tag{6}$$

The scalar damage variable D_X was used as an internal variable to represent the material degradation. The weakening function $w(D_X) = 1 - D_X^\beta$ is adopted to describe the damage effect on the macroscopic strength:

$$\dot{D}_X = m \left(\frac{\bar{\epsilon}_p}{\epsilon_f(p, \theta_L)} \right)^{m-1} \frac{\dot{\bar{\epsilon}}_p}{\epsilon_f(p, \theta_L)} \quad \text{and} \quad \bar{\sigma} = \left(1 - D_X^\beta \right) \sigma_M \tag{7}$$

where β is the weakening exponent, $\bar{\epsilon}_p$ is the equivalent plastic strain, σ_M is the flow stress of undamaged material.

2.3 Micromechanics-based models

The yield function of the GTN model ([9]) writes:

$$\phi = \left(\frac{\bar{\sigma}}{\sigma_0} \right)^2 + 2q_1 f^* \cosh(-\frac{3q_2}{2} \frac{p}{\sigma_0}) - 1 - q_3 f^{*2} = 0 \tag{8}$$

σ_0 is the flow stress of matrix material; q_1, q_2, $q_3 = (q_1)^2$ are material constants; f^* is the effective void volume fraction, which accounts for the voids' linkage:

$$f^* = \begin{cases} f & ,if \quad f < f_c \\ f_c + \frac{f_u^* - f_c}{f_f - f_c}(f - f_c) & ,if \quad f \geq f_c \end{cases} \tag{9}$$

where f_c represents the critical value of f at which void coalescence begins, f_f its value at ductile failure, and $f_u^* = \frac{q_1 \pm \sqrt{q_1^2 - q_3}}{q_3}$ the corresponding value of f^* at failure. The evolution of void volume fraction is described as:

$$\dot{f} = \dot{f}_{\text{nucleation}} + \dot{f}_{\text{growth}} \tag{10}$$

where $\dot{f}_{\text{growth}}$ is defined as $\dot{f}_{\text{growth}} = (1 - f)\text{trace}(\dot{\boldsymbol{\epsilon}}_p)$ and $\dot{f}_{\text{nucleation}}$ is often described by a Gaussian curve introduced by [10]:

$$\dot{f}_{\text{nucleation}} = \frac{f_N}{S_N \sqrt{2\pi}} \exp\left[-\frac{1}{2}\left(\frac{\bar{\epsilon}_p - \epsilon_N}{S_N}\right)^2\right] \dot{\bar{\epsilon}}_p = A\left(\bar{\epsilon}_p\right)\dot{\bar{\epsilon}}_p \tag{11}$$

Xue proposed a new damage variable (D) which accounts for void shearing damage:

$$\dot{D} = \delta_D \left(q_1 \dot{f} + \dot{D}_{\text{shear}}\right) \tag{12}$$

where δ_D is the damage rate coefficient. For the GTN model, which accounts for coalescence (i.e. using f_c to define the start of coalescence stage), this coefficient is defined as:

$$\delta_D = \begin{cases} 1 & ,if \quad D \leq D_c = q_1 f_c \\ \frac{f_u^* - f_c}{f_f - f_c} & ,if \quad D_c < D \leq 1 \end{cases} \tag{13}$$

$$\dot{D}_{\text{shear}} = q_3^* f^{q_4} \bar{\epsilon}_p \dot{\bar{\epsilon}}_p g_\theta \quad \text{where} \quad g_\theta = 1 - \frac{6|\theta_L|}{\pi} \tag{14}$$

In addition to this modification, in order to account for the influence of the stress triaxiality on the nucleation process, Cao et al. [2] proposed a formulation for the strain at maximum nucleation ϵ_N as:

$$\epsilon_N = \epsilon_{N_0} \exp(-B\eta) \tag{15}$$

where η is the stress triaxiality, which can be taken as the initial stress triaxiality if the loading is nearly proportional; B and ϵ_{N_0} are two parameters to be identified. This modification allows the void nucleation process to take place earlier at high stress triaxialities, which is materialized by the experiments of Kao et al. [11]. The GTN model with the modification proposed by [6] and [2] is called the modified GTN model in the present study.

2.4 Implementation and calibration

All models were implemented in Forge®, an implicit, 3D Finite Element software based on a mixed velocity-pressure formulation using mini-elements ([12, 13]). Identification of the parameters of the models above, plus those describing work-hardening, has been performed using a set of experiments covering the plane ($\eta, \bar{\theta}$): cylinder compression (-1/3;-1); torsion (0;0); plane-strain, flat grooved specimen ($\approx$ 2/3-1;0); round and notched bar tension (1/3-2/3;1). For Gurson-Tvergaard-Needleman - like models, X-Ray microtomography has been used also to identify nucleation parameters and porosity at fracture ([2]). The calibration of all models were based on inverse analyses using multi-objective automatic optimization program ([14]).

3 Examples of applications

In this section, the above-mentioned models are compared in terms of damage prediction in two industrial forming processes: wire drawing and wire flat rolling (high carbon steel). In addition, the Lemaitre and B&W models were also applied to predict fracture in rolling of stainless steel wire.
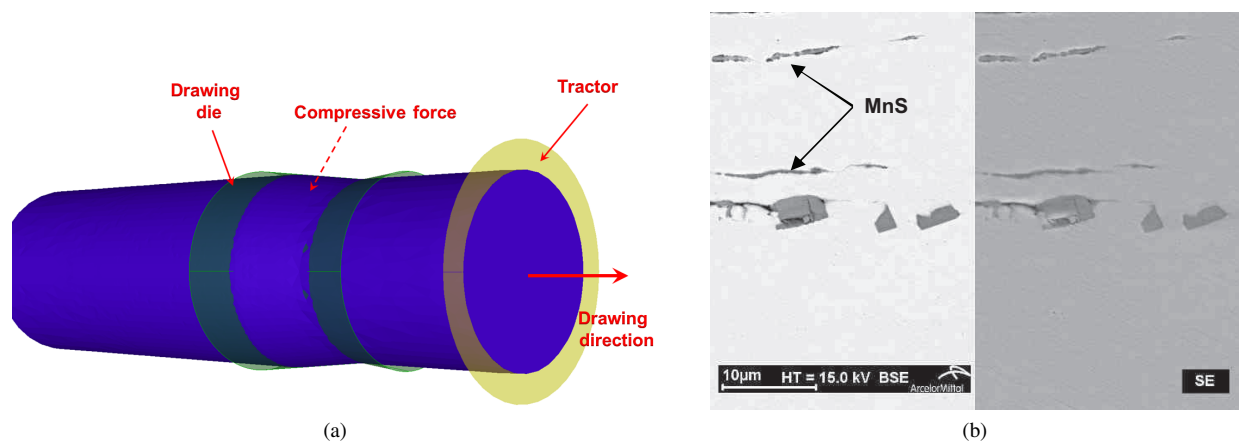
3.1 Wire drawing process

Figure 1: (a) Schematic of drawing; and (b) SEM images of microstructure in the drawing direction (horizontal direction) after four passes wire drawing [15]).

Fig. 1a shows the schematic of the studied wire drawing process. Fig. 1b shows the damage state observed after four passes of drawing, near the wire center (total average deformation $\bar{\epsilon} \approx 0.81$). As can be observed, deformable inclusions are oriented following the drawing direction. At this stage, inclusion cracking is also observed but negligible.

For the wire drawing process, most models predict higher damage in the wire core than in the wire skin ([15]). In experiment, fracture occured in the wire core after 14 drawing passes. Fig. 2 shows damage distributions on the longitudinal and transverse cross sections, at the second pass, which confirm high localization of damage in the wire core (except the modified GTN model). Moreover, between the Lemaitre and Xue coupled models, a stronger localization in the wire center can be observed with the Lemaitre model, while for the Xue model, damage changes gradually from the wire core to the wire surface. In addition, regarding the LEL model, which accounts for the influence of the Lode parameter, damage accumulation is also predicted on wire surface, although less intense than in the wire core. It means that, for the models based on both the Lode parameter and the stress triaxiality (i.e. B&W, Xue and LEL), the influence of shear, which is maximum on the wire surface, is accounted for with a stronger weight than for the stress triaxality-based model (e.g. Lemaitre). Moreover, in the working zone, since the stress triaxiality in the wire surface is negative, damage accumulation predicted by the stress triaxality-based Lemaitre model is not noticeable at this location. It should be noted that, in [15], results revealed that only the GTN model gives a satisfactory results regarding the prediction of the moment of fracture (after 13 passes).

3.2 Wire flat rolling

Fig. 3a represents the schematic of the studied wire flat rolling process. As the wire passes through the rolls, all material points across the width experience some tendency to expand laterally (transverse direction); this is called *"spread"*. The edges are thus strained in tension, which may lead to edge cracking. The edge center tends to expand laterally more than the upper and lower surfaces, which produces barreled edges similar to those observed in compression of a cylinder. Therefore, theoretically, in this process, the barreled areas are critical zones where cracks tend to initiate first. An experimental study of damage in rolling process was performed in [16]. Damage was identified at a microscopic scale through SEM observations, which showed decohesion around non deformable inclusions (matrix-inclusion debonding) and fragmentation of deformable inclusions. The FEM analysis of the strain map was also presented, which showed a localization in form of a cross (the *"blacksmith cross"*). This strain localization may explain the evolution of microstructure during rolling (see [16] for more details). The experimental sketch of damage, superposed on a strain map obtained with FEM analysis, is presented in Fig. 3b. Since this process involves a global vertical compression with a significant transverse flow, the expansion of decohesion thus follows the transverse direction. Moreover, the inclusions located in the branches of the blacksmith cross seem to have a preferential orientation due to rotation associated with shear strain in this area. The authors mentioned a higher void density as well as a higher flattening of cavities in the wire core than in the edge. Therefore, from this experimental observation, the rolling process principally affects the voids in the wire core and on the blacksmith cross. Voids located in the barreled zone were also expanded laterally due to rolling, but the expansion is smaller.

In rolling (Figs. 4 and 5), Lemaitre's model gives maximum damage on the edge, with a small secondary peak at the
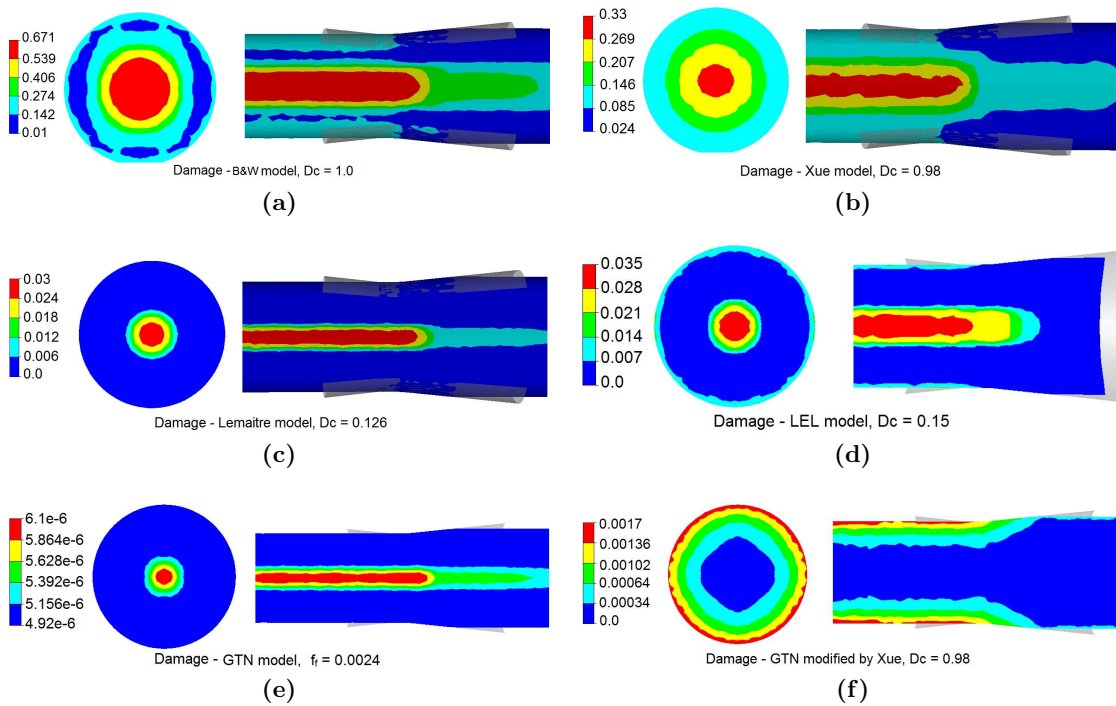
Figure 2: Damage at steady state of second drawing pass for six damage models: (a) Bai & Wierzbicki, (b) Xue, (c) Lemaitre, (d) LEL, (e) GTN and (f) modified GTN by Xue. The values are represented on the longitudinal and transverse cross sections.
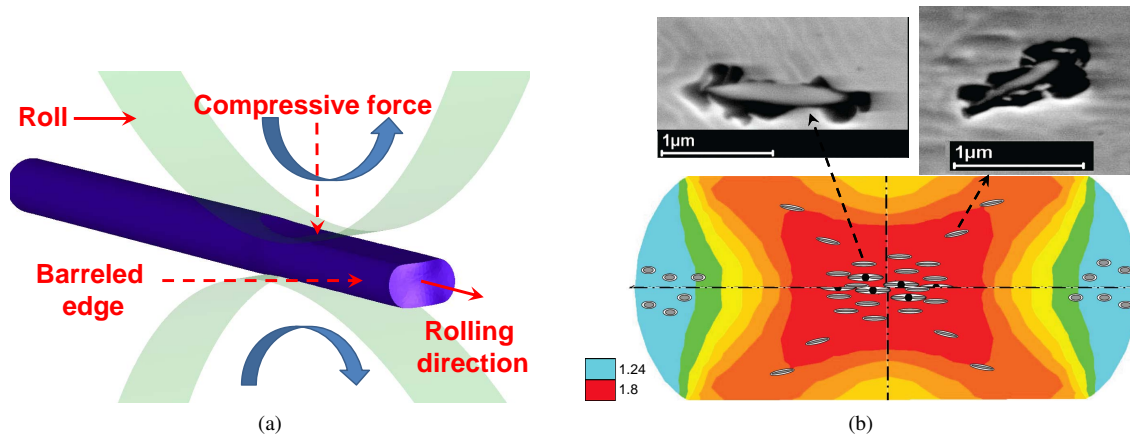

Figure 3: (a) Schematic of wire flat rolling; and (b) sketch of the damage state at the end of rolling superimposed to strain map obtained by FEM analysis (color). The zoomed pictures show flattened deformable inclusions in the wire core and in the blacksmith cross (SEM pictures - adapted from [16]).

center corresponding to the heritage of wire-drawing. On the contrary, its shear-enhanced version ("LEL") depicts the blacksmith's cross. The same difference can be found between Gurson-Tvergaard-Needleman ("Porosity") and shear-enhanced Gurson-Tvergaard-Needleman ("Dx-GTN") (in experiments, the most dangerous zones are the center and the blacksmith cross - see ([17], or [18]). The Bai & Wierzbicki model ("B&W") is close to Gurson-Tvergaard-Needleman, whereas Xue's model resembles the enhanced Lemaitre model

3.3 Fracture prediction in wire round rolling

The studied rolling process consists of 5 "passes", each pass involving 2 stands (3+3 rolls or 2+2 rolls). The first pass uses the 3+3 technology (see Fig. 6a), where 2 stands of 3 rolls are set next to each other. For each stand, one roll makes an angle
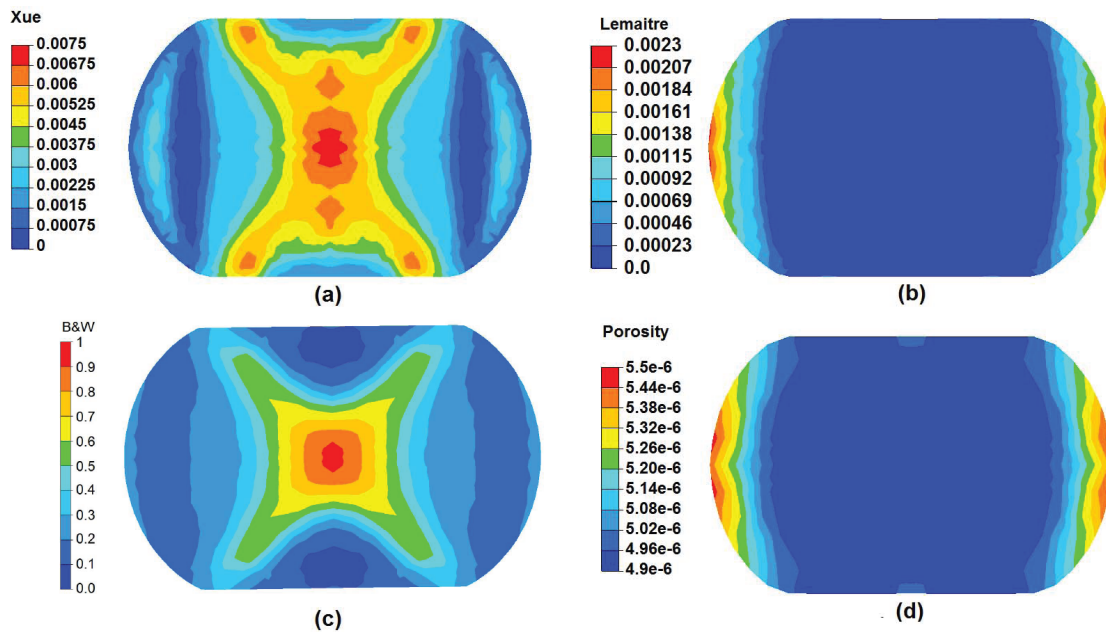
Figure 4: Damage on a cross section perpendicular to the rolling direction with different models: (a) Xue, (b) Lemaitre, (c) B&W, and (d) GTN.
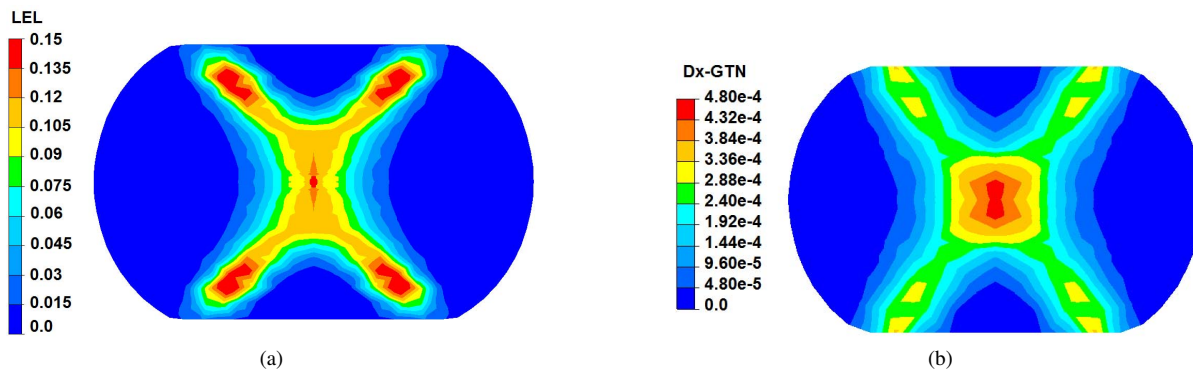

Figure 5: Damage on a cross section perpendicular to the rolling direction with two enhanced models: (a) LEL and (b) modified GTN by Xue.

of 120° with another. For the other four rolling passes, the 2+2 rolls are used, which consists of one horizontal stand and one vertical stand of 2 rolls (see Fig. 6b). Figs. 6a and 6b represent numerical models for 3+3 and 2+2 technologies respectively. Only a part of wire about 15 cm long was modeled to reduce CPU time. The mesh of the wire is also presented in Fig. 6c.

(a) 3+3 technology.   (b) 2+2 technology.   (c) Mesh used for steel wire before rolling.
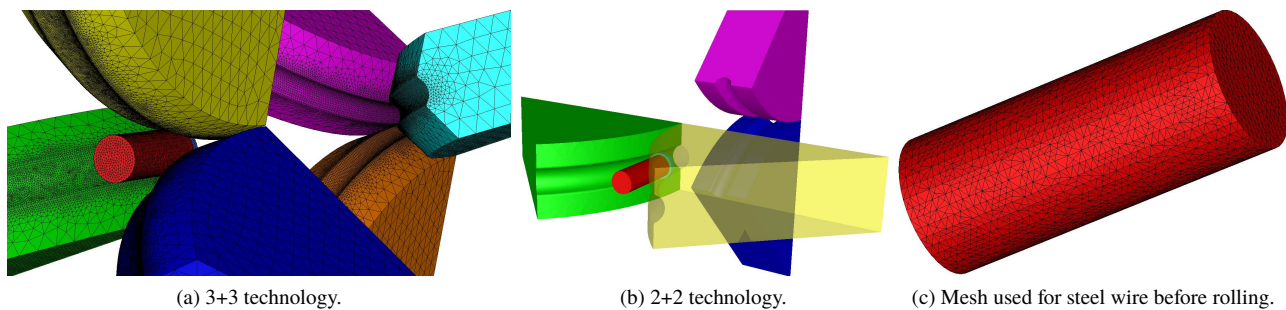
Figure 6: The studied rolling mills and mesh used.

Fig. 7 shows the comparison between cracks observed at the outlet in wire round rolling process on a stainless steel

obtained from experiment (Fig. 7a) and from numerical prediction with the Lemaitre-type model (Fig. 7b). For this process, fracture occurs on the wire surface. It should be noted that, in [18, 19], the authors showed that, both the Lemaitre-type and B&W models give correct prediction for both fracture location and the instant of fracture for this process.

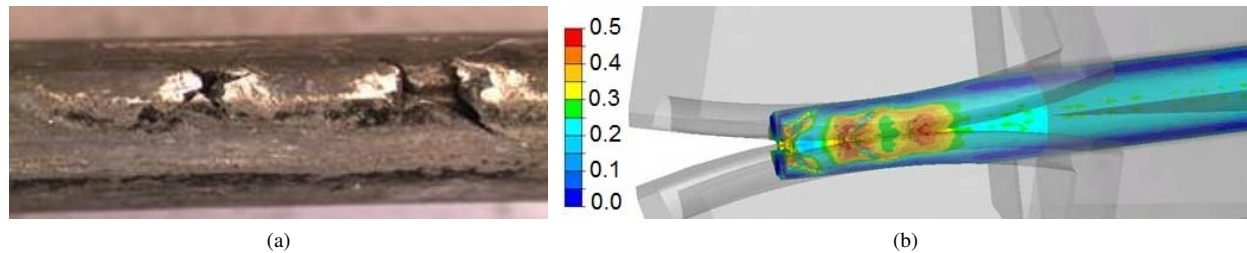(a)   (b)

Figure 7: (a) Experimental observations of cracks on the surface of rolled wire; (b) numerical prediction obtained with the Lemaitre-type model, showing cracks at outlet ([18].

4. Closure remark

Six damage models from the recent literature have been implemented, their parameters identified from experiments, and their performance tested on different cold forming schedules. Note that the sets of parameters identified by laboratory mechanical tests have been used "as is", without any modification, to study wire-drawing and wire rolling. The experimental trends in terms of time and location of failure have been checked. In the wire drawing of patented high carbon steel, the Gurson-Tvergaard-Needleman model is the one which best fits measurements. Other models predict a largely premature failure (although critical positions were accurately predicted). Regarding rolling process, experimental void density maps can be reproduced only with shear-emphasizing damage models. It is quite difficult to obtain a good balance between the lateral surfaces (low but non negligible porosity), the center (largest density) and the arms of the blacksmith's cross (intermediate). Again, Gurson-Tvergaard-Needleman is globally the best if used with shear-enhancement (here, the Xue phenomenological formulation). Another application for round-rolling on a stainless steel reveals that both the stress-triaxiality based (Lemaitre) and Lode and triaxiality based models (B&W) provided accurately results in terms of fracture prediction in the zone of high lateral expansion (positive stress-triaxiality zone). These results suggest that, for the process with high triaxiality zone, triaxiality-based models could give correct predictive results. However, regarding processes involving strong shear, models should account for both stress triaxiality and Lode parameter. In addition, as can be observed, voids are elongated in the drawing direction in the wire drawing process and voids are flattened and rotated following the shear band in the rolling process. The GTN model with underlying assumption of spherical cavities shows its limitation in these cases. The use of a purely micromechanical model ([20, 21]), which accounts for void shape change and void rotation, is of great interest for future studies.

References

[1] T.-S. Cao, C. Bobadilla, P. Montmitonnet, and P.-O. Bouchard. On the development and identification of phenomenological damage models - Application to industrial wire drawing and rolling processes. *Key Engineering Materials*, 554 - 557:213–226, 2013.

[2] T.-S. Cao, E. Maire, C. Verdu, C. Bobadilla, P. Lasne, P. Montmitonnet, and P.-O. Bouchard. Characterization of ductile damage for a high carbon steel using 3d x-ray micro-tomography and mechanical tests - application to the identification of a shear modified gtn model. *Computational Materials Science*, 84:175 – 187, 2014.

[3] Y. Bai and T. Wierzbicki. A new model of metal plasticity and fracture with pressure and Lode dependence. *International Journal of Plasticity*, 24(6):1071 – 1096, 2008.

[4] J. Lemaitre. Local approach of fracture. *Engineering Fracture Mechanics*, 25(5-6):523–537, 1986.

[5] T.-S. Cao, J.-M. Gachet, P. Montmitonnet, and P.-O. Bouchard. A Lode-dependent enhanced Lemaitre model for ductile fracture prediction at low stress triaxiality. *Engineering Fracture Mechanics*, 124 - 125(0):80 – 96, 2014.

[6] L. Xue. Damage accumulation and fracture initiation in uncracked ductile solids subject to triaxial loading. *International Journal of Solids and Structures*, 44(16):5163 – 5181, 2007.

[7] Y. Bao and T. Wierzbicki. On fracture locus in the equivalent strain and stress triaxiality space. *International Journal of Mechanical Sciences*, 46(1):81–98, 2004.

[8] Y. Lou, J. W. Yoon, and H. Huh. Modeling of shear ductile fracture considering a changeable cut-off value for stress triaxiality. *International Journal of Plasticity*, 54(0):56 – 80, 2014.

[9] V. Tvergaard and A. Needleman. Analysis of the cup-cone fracture in a round tensile bar. *Acta Metallurgica*, 32(1):157 – 169, 1984.

[10] C. C. Chu and A. Needleman. Void nucleation effects in biaxially stretched sheets. *Journal of Engineering Materials and Technology*, 102(3):249–256, 1980.

[11] A. S. Kao, H. A. Kuhn, O. Richmond, and W. A. Spitzig. Tensile fracture and fractographic analysis of 1045 spheroidized steel under hydrostatic pressure. *Journal of Materials Research*, 5(1):83–91, 1990.

[12] T.-S. Cao, P. Montmitonnet, and P.-O. Bouchard. A detailed description of the Gurson-Tvergaard-Needleman model within a mixed velocity-pressure finite element formulation. *International Journal of Numerical Methods in Engineering*, 96(9):561–583, 2013.

[13] T.-S. Cao. Numerical simulation of 3D ductile cracks formation using recent improved Lode-dependent plasticity and damage models combined with remeshing. *International Journal of Solids and Structures*, 51(13):2370 – 2381, 2014.

[14] T.-S. Cao, A. Gaillac, P. Montmitonnet, and P.-O. Bouchard. Identification methodology and comparison of phenomenological ductile damage models via hybrid numerical-experimental analysis of fracture experiments conducted on a zirconium alloy. *International Journal of Solids and Structures*, 50(24):3984 – 3999, 2013.

[15] T.-S. Cao, C. Bobadilla, P. Montmitonnet, and P.-O. Bouchard. A comparative study of three ductile damage approaches for fracture prediction in cold forming processes. *Journal of Materials Processing Technology*, 216(0):385 – 404, 2015.

[16] T. Massé, Y. Chastel, P. Montmitonnet, C. Bobadilla, N. Persem, and S. Foissey. Mechanical and damage analysis along a flat-rolled wire cold forming schedule. *International Journal of Material Forming*, 5(2):129–146, 2012.

[17] T. Massé. *Study and optimization of high carbon steel flat wires*. PhD thesis, Ecole Nationale Supérieure des Mines de Paris, 01 2010.

[18] T.-S. Cao. *Modeling ductile damage for complex loading paths*. PhD thesis, Ecole Nationale Supérieure des Mines de Paris, 10 2013.

[19] T.-S. Cao, C. Vachey, P. Montmitonnet, and P.-O. Bouchard. Comparison of reduction ability between multi-stage cold drawing and rolling of stainless steel wire - Experimental and numerical investigations of damage. *Journal of Materials Processing Technology*, 217(0):30 – 47, 2015.

[20] K. Danas and N. Aravas. Numerical modeling of elasto-plastic porous materials with void shape effects at finite deformations. *Composites Part B: Engineering*, 43(6):2544 – 2559, 2012. Homogenization and Micromechanics of Smart and Multifunctional Materials.

[21] T.-S. Cao, M. Mazière, K. Danas, and J. Besson. A model for ductile damage prediction at low stress triaxialities incorporating void shape change and void rotation. *International Journal of Solids and Structures*, 63(0):240 – 263, 2015.